Research Paper
Computational Methods for Differential Equations
http://cmde.tabrizu.ac.ir
Vol. 13, No. 3, 2025, pp. 870-884
DOI:10.22034/cmde.2024.59036.2504

Mathematical modeling of COVID-19 with a constant spatial diffusion term in Ghana

Vivian Osei-Buabeng[1,*], **Albert Attakora Frimpong**[2], **and Benedict Barnes**[1]
[1]Department of Mathematics, College of Science, Kwame Nkrumah University of Science and Technology, Ghana.
[2]Kwame Nkrumah University of Science and Technology Senior High School, Ghana.

Abstract

The purpose of this study is to develop a mathematical model that incorporates a diffusion term in one dimension in the dynamics of coronavirus disease-19 (COVID-19) in Ghana. A reaction-diffusion model is derived by applying the law of conservation of matter and Fick's law, which are fundamental theorems in fluid dynamics. Since COVID-19 is declared to be a pandemic, most African countries are affected by the negative impacts of the disease. However, controlling the spread becomes a challenge for many developing countries like Ghana. A lot of studies about the dynamics of the infection do not consider the fact that since the disease is pandemic, its model should be spatially dependent, therefore failing to incorporate the diffusion aspect. In this study, the local and global stability analyses are carried out to determine the qualitative solutions to the SEIQRF model. Significant findings are made from these analyses as well as the numerical simulations and results. The basic reproduction number (R_o) calculated at the disease-free fixed point is obtained to be $R_o \approx 2.5$, implying that, an infectious individual is likely to transmit the coronavirus to about three susceptible persons. A Lyapunov functional constructed at the endemic fixed point also explains that the system is globally asymptotically stable, meaning that COVID-19 will be under control in Ghana for a long period of time.

Keywords. Spatial spread, Lyapunov function, Reaction-diffusion model, Wave speed.
2010 Mathematics Subject Classification. 65L05, 34K06, 34K28.

1. Introduction

A disease like pneumonia from an unknown cause broke out in Wuhan city in China on 31st December 2019. As the Chinese authorities could not figure out the causal virus of this pneumonic disease [13], they reported it to the World Health Organization [5]. In a week's time, that is, January 7, 2020, the virus was identified to be a new coronavirus called (2019 Cov) disease and later named the disease COVID-19. Coronavirus disease is caused by severe acute respiratory syndrome coronavirus-2. It is believed to be the third human coronavirus disease to outbreak after SARS-CoV and MERS-CoV which occurred in 2002 and 2012 respectively [22]. As the name of the virus implies, it affects the respiratory system of an individual, which causes them to exhibit mild to severe symptoms like loss of smell and taste, headaches, dry cough, and difficulty in breathing.

Coronavirus is usually transmitted through human-to-human contact, whereby if a person interacts with the droplets of an infected person, they may also get infected [13]. COVID-19 started as an epidemic in Wuhan, China. It invaded throughout China within a short period of time. Strict control measures were adhered to; some of these were closure of schools, businesses, and other social places; wearing of face masks; and regular washing of hands were the hygienic protocols of the time [16]. Wuhan, a city of about 11 million people, was put under total lock-down; COVID-19 patients were given treatment as they were put under mandatory isolation [17].

Unfortunately, China alone could not contain the disease; therefore, the infection spread to many other parts of the world. By March 2020, China had recorded about 81,394 cases with 3,281 deaths. South Korea's first confirmed case was believed to have occurred in Church. The USA had recorded about 6,368 positive cases, with 1,681 deaths [2]. In

Received: 30 October 2023 ; Accepted: 11 August 2024.
∗ Corresponding author. Email: vivianobuabeng19@gmail.com.

Europe, every country had confirmed cases, and all have reported at least one death. Italy confirmed 28,126 positive cases, of which 3,418 were deaths. Due to this, Italy was termed the epicenter of the infection. In Africa, South Africa had recorded 202 cases, Nigeria, 2 cases, Togo, 1 case, and Ghana also got its share of the infection with 2 confirmed cases in March 2020. As 26th of March, 2020, 503,274 confirmed cases with 22,342 deaths were recorded cumulatively worldwide [20]. Nevertheless, Ghana also got its share of the infection in March 2020.

According to a report from the World Health Organization (WHO), the world recorded a total of 1,353,361 infected cases with 79,235 deaths, representing 5.85% from the onset of the outbreak [20]. Due to the alarming impact of the disease across the world, the WHO declared COVID-19 a global pandemic. Within two months from the onset of the outbreak, Ghana had recorded about 12,000 positive cases through contact tracing, out of which 49 were deaths [2]. Some control measures like social and physical distancing, closure of schools, wearing of face masks, and banning of social gatherings were adopted by some stakeholders and the Ghana government [7]. COVID-19 has caused many lives and brought immense negative impact on the global economy. Now Ghana is still battling with coronavirus as well as the world at large, even as we are experiencing other forms of this pandemic, like the Delta and the Omicron variants. Thus, there is the need for intensive research on COVID-19 by looking at it from the pandemic view and not the epidemic.

This study seeks to dispute the established claim from some studies of COVID-19 as an epidemic [17]. As the diffusion term is incorporated in the model, it makes the dynamics of the model spatially dependent, thus revealing a more relevant view that COVID-19 is a pandemic but not an epidemic [23]. This is because, as people keep moving from one position or space to another, the disease also keeps spreading, obviously revealing spatial, dependence nature of COVID-19.

The mathematical model developed to describe the dynamics of COVID-19 includes a diffusion term in one dimension. The study also determines the qualitative and quantitative solutions of the model. The stability analysis, which determines the qualitative solution of the model, calls for the need to also check for any parameter that has a greater or lesser effect on the basic reproduction number ($\mathcal{R}_o$) [21].

This study makes some significant contributions to the mathematical modeling of COVID-19. The particular significance of this study basically lies in the law of conservation of matter, Fick's law, and the divergence theorem, which have been extensively applied. In the study, the reaction-diffusion equation was birthed from these fundamental theorems of fluid dynamics upon which the SEIQRF model was built. The SEIQRF model developed is a mixture of nonlinear partial and ordinary differential equations. In the model, the constant diffusion term is attached to the spatially dependent population states, which are Susceptible (S), Exposed (E), and Infectious (I). However, the remaining three states, namely Quarantined (Q), Recovered (R), and Fatality (F), are assumed to depend on only time. Local and global stability analyses are carried out as well, where the next-generation matrix is obtained from the SEIQRF model and used to derive the basic reproduction number R_o 9.

The new Lyapunov functions constructed at the endemic fixed point gave an insight about the fate of COVID-19. The Lyapunov functions as well as the Routh-Hurwitz criterion generated are able to determine the global asymptotic stability of the system. Which actually means that, COVID-19 will be under control with time in Ghana. The numerical simulations made in this work also depict a positive result that the disease will decay with time. Most COVID-19 researchers tailored the dynamics of the coronavirus as though its epidemiology is an epidemic. But as the infection continues to spread from one concentrated region to a low-infection or no-infection region, its study ceases to be an epidemic but rather a pandemic.

The objective in the paper of [1] was to determine the global stability of constant fixed-point solutions to the reaction-diffusion system with the Neumann boundary conditions. They constructed a Lyanpunov functional for delay partial differential equations or partial differential equations.

In the same paper [1], they modeled COVID-19 as an SEIR model in Pakistan. They added the quarantined, isolated, and asymptomatic classes to their model compartments. The dynamics of the COVID-19 outbreak in Pakistan were qualitatively different before and after the lockdown was eased. They estimated the value of the R_0 in Pakistan before lockdown and after lockdown of the outbreak, noting that during this time no medication was available. They projected the infection curve considering minimal intervention as well as various control strategies.

In [17], the authors simulated the outbreak in Wuhan using a deterministic stage-structured SEIR model over a year period, during which the modeled outbreak peters out. They failed to incorporate the diffusion term since, at the time this study was embarked on, the WHO had declared COVID-19 a pandemic. However, in [23], the authors considered the diffusion aspect in their model. They felt the need to prove the existence of the wavefront solutions of their model and hence considered equal diffusivity coefficients for the three compartments.

2. Model description and stability analysis

This section explains the description of both the model and the compartmental model (flowchart). The analysis of some stability methods used in the study is also discussed here.

2.1. **Assumptions of the Study.** The assumptions of the study are:

(1) The diffusivity coefficient D is the same for susceptible, exposed, and infectious classes.
(2) There is homogeneous mixing of COVID-19 patients and susceptibles.
(3) The spatial spread is in one dimension.
(4) Recovered persons do not get reinfected.

2.2. **Construction of a COVID-19 mathematical model.**

The mathematical model in this study was birthed out of the spirits of Kermack-Mckendrick and reaction-diffusion models [3, 15]. A COVID-19 model in a human population was constructed and analyzed. The total human population at time t, denoted by N, is stratified into six mutually exclusive sub-populations, namely, susceptible $S(t)$, exposed $E(t)$, infectious $I(t)$, quarantined $Q(t)$, detected recovered $R(t)$ and fatality $F(t)$ sub-populations. Thus, the total human population is given by $N = S(t) + E(t) + I(t) + Q(t) + R(t) + F(t)$.

Theorem 2.1. *From Fick's law, the amount of flow per unit area (J) of a material (density of human beings or chemical) is proportional to the gradient of the concentration (ϕ) of the material.*

$$J = -D\frac{\partial \phi}{\partial x}, \tag{2.1}$$

where D is the coefficient of diffusion.

Theorem 2.2. *Also, from the law of conservation of matter, the rate of change of the amount of material in volume V is equal to the rate of flow of material across the surface area S into V plus the material created in V. Thus*

$$\frac{\partial}{\partial t}\int\int\int_V \phi(x,t)dV = -\int\int_S J \cdot dS + \int\int\int_V f(\phi, x, t)dV. \tag{2.2}$$

Theorem 2.3. *Suppose that $Q \subset R^3$ is bounded by the closed surface ∂Q and $n(x, y, z)$ denotes the exterior unit normal vector to ∂Q. Then if the component of $F(x, y, z)$ contains the first partial derivative in Q*

$$\int\int_{\partial Q} F \cdot ndS = \int\int\int_V \nabla \cdot FdV. \tag{2.3}$$

Eq. (2.3) is called the divergence theorem, and it is used here because it allows for the conversion of surface integrals into volume integrals.

Remark 2.4. F is a continuous vector field on the surface S with the unit normal vector n. Thus, the surface integral of F over S is given by

$$\int\int_S F \cdot dS = \int\int_S F \cdot ndS. \tag{2.4}$$

The integral in (2.4) is the flux of F across the surface S, and it simply means the surface integral of F over S is equal to the surface integral of its normalized component n over surface S. Now in (2.4), the integral on the RHS has n because the surface is in the direction of n, whose magnitude is one. Similarly, the first integral on the RHS of (2.2) is also the flux of J and takes the form of (2.4). Therefore, Eq. (2.3) can be applied.

Applying the divergence theorem to the first term on the RHS of (2.2) yields

$$\int\int\int_V \frac{\partial}{\partial t}\phi(x,t)dV + \int\int\int_V \nabla\cdot J dV - \int\int\int_V f(\phi,x,t)dV = 0.$$

By the linearity of the integral operator

$$\int\int\int_V \left(\frac{\partial}{\partial t}\phi(x,t) + \nabla\cdot J - f(\phi,x,t)\right)dV = 0,$$

$$\frac{\partial\phi(x,t)}{\partial t} = f(\phi,x,t) - \nabla\cdot J. \tag{2.5}$$

Substituting Eq. (2.1) into (2.5) gives:

$$\frac{\partial\phi(x,t)}{\partial t} = f(\phi,x,t) - \nabla\cdot\left(-D\frac{\partial\phi}{\partial x}\right),$$

hence

$$\frac{\partial\phi}{\partial t} = f(\phi) + D\frac{\partial^2\phi}{\partial x^2}. \tag{2.6}$$

Eq. (2.6) is the reaction-diffusion equation, where $f(\phi)$ is the reaction and $D\frac{\partial^2\phi}{\partial x^2}$ is the diffusion. Now the mathematical model governing the dynamics of COVID-19 in humans is described by the system of nonlinear partial and ordinary differential equations given in (2.7), which takes the form of the reaction-diffusion equation.

$$\begin{aligned}
\frac{\partial S}{\partial t} &= \alpha N - \frac{\beta S}{N}(I+Q) - \mu S + D\frac{\partial^2 S}{\partial X^2},\\
\frac{\partial E}{\partial t} &= \frac{\beta S}{N}(I+Q) - (\gamma+\sigma+\mu)E + D\frac{\partial^2 E}{\partial X^2},\\
\frac{\partial I}{\partial t} &= \gamma E - (\psi+\delta+\kappa)I + D\frac{\partial^2 I}{\partial X^2},\\
\frac{dQ}{dt} &= \psi I + \sigma E - (\epsilon+\mu+\omega)Q,\\
\frac{dR}{dt} &= \epsilon Q + \kappa I - \mu R,\\
\frac{dF}{dt} &= \delta I + \omega Q,
\end{aligned} \tag{2.7}$$

where $N = S(t) + E(t) + I(t) + Q(t) + R(t) + F(t)$.

2.3. **Description of the model.** The model can be classified into six compartments, as seen in Figure 1. The S class in this figure, denoting the susceptible class, contains persons who have never contracted COVID-19 but are likely to be infected. New births are born into this group by the birth rate α, and μ is the natural death rate at which the susceptible persons die of any other conditions. Persons who get infected as a result of an interaction with COVID-19 patients are moved from the susceptible group by the rate β into the exposed class (E) [17].

After the 10- to 14-days incubation period [8], exposed individuals begin to show symptoms and can also infect others. The rate at which this happens is γ. Hence they are classified as the infectious (I). The quarantined class (Q) contains infected and infectious individuals that either self-isolate or are put under mandatory quarantine by σ and ψ rates, respectively [12]. Some COVID-19 patients may recover naturally, while others may undergo treatment before recovering. These persons belong to the recovered class (R), and the rates at which this is done are ϵ and κ. Patients that lose their lives by δ and ω rates belong to the fatality class (F). All arrows indicate transition from one disease status to another. Table 1 illustrates the symbols used to define the previous disease states and parameters. Table 2 illustrates the initial population and proportions of each state.

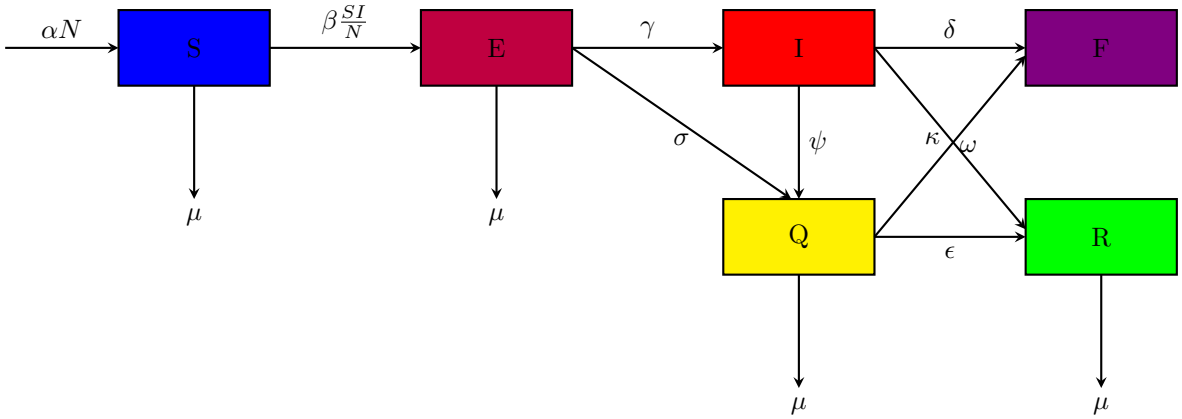

FIGURE 1. Compartmental diagram for the COVID-19 model in Eq. (2.7).

TABLE 1. Representation of the assigned symbols to the various disease states and parameters.

Symbols	Description
$S(0)$	Initial susceptible individuals
$E(0)$	Initial exposed individuals
$I(0)$	Initial infected individuals
$Q(0)$	Initial quarantined individuals
$R(0)$	Initial recovered individuals
$F(0)$	Initial deceased individuals
α	New birth rate
β	Transmission rate from infected persons
γ	Rate at which exposed persons move into the infectious class
σ	Rate at which exposed persons get self-isolation
ψ	Rate at which detected infected persons are quarantined
ϵ	Recovery rate of being quarantined
κ	Recovery rate without being quarantined
δ	Disease-induced death rate from infectious class
ω	Disease-induced death rate from quarantined class
μ	Natural death rate

2.4. **Local stability analysis of the model.** Local stability of the model seeks to determine the fixed points of the six states or compartments [11]. Here qualitative solutions are found at the disease-free fixed point with and without the diffusion speed c [15]. This is relevant when the initial conditions of the states are in proportion. Doing this requires a set of dimensionless parameters, which are put in Eq. (2.8).

$$
\begin{aligned}
&s = \frac{S(X,t)}{N},\ e = \frac{E(X,t)}{N},\ i = \frac{I(X,t)}{N},\ q = \frac{Q(t)}{N},\ r = \frac{R(t)}{N},\ f = \frac{F(t)}{N},\\
&a_1 = \frac{\beta}{\alpha}, a_2 = \frac{\mu}{\alpha}, a_3 = \frac{\gamma}{\alpha}, a_4 = \frac{\sigma}{\alpha}, a_5 = \frac{\psi}{\alpha},\ a_6 = \frac{\delta}{\alpha}, a_7 = \frac{\kappa}{\alpha}, a_8 = \frac{\epsilon}{\alpha},\\
&a_9 = \frac{\omega}{\alpha},\ x = X\left(\frac{\alpha}{D}\right)^{1/2},\ \tau = \alpha t,\ [15].
\end{aligned}
\tag{2.8}
$$

Hence, the required non-dimensionalized system gives the equations below, which will be converted into first-order scalar differential equations.

$$\begin{aligned}
\frac{\partial s}{\partial \tau} &= 1 - a_1 s(i+q) - a_2 s + \frac{\partial^2 s}{\partial x^2},\\
\frac{\partial e}{\partial \tau} &= a_1 s(i+q) - (a_2 + a_3 + a_4)\, e + \frac{\partial^2 e}{\partial x^2},\\
\frac{\partial i}{\partial \tau} &= a_3 e - (a_5 + a_6 + a_7)\, i + \frac{\partial^2 i}{\partial x^2},\\
\frac{dq}{d\tau} &= a_5 i + a_4 e - (a_2 + a_8 + a_9)\, q,\\
\frac{dr}{d\tau} &= a_8 q + a_7 i - a_2 r,\\
\frac{df}{d\tau} &= a_6 i + a_9 q.
\end{aligned} \tag{2.9}$$

If invaders traveled into the country with constant speed, then it implies $z(x,\tau) = x - c\tau$, and $s(z) = s(x,\tau)$ [15].

$$\Rightarrow \frac{ds}{dz} = \frac{\partial s}{\partial x},$$

$$\Rightarrow \frac{d^2 s}{dz^2} = \frac{\partial^2 s}{\partial x^2}, \tag{2.10}$$

$$\frac{\partial s}{\partial \tau} = -c\frac{ds}{dz}. \tag{2.11}$$

Substituting (2.10) and (2.11) into (2.9) yields

$$-c\frac{ds}{dz} = 1 - a_1 s(i+q) - a_2 s + \frac{d^2 s}{dz^2}\ . \tag{2.12}$$

Again, setting

$$s(z) = u_1(z), \tag{2.13}$$

and

$$\frac{ds}{dz} = u_2(z), \tag{2.14}$$

differentiating (2.13) gives

$$\frac{ds}{dz} = \frac{du_1}{dz}, \quad \Rightarrow \quad \frac{du_1}{dz} = u_2. \tag{2.15}$$

Differentiating (2.14)

$$\frac{d^2 s}{dz^2} = \frac{du_2}{dz},$$

gave the first scalar differential equation in (2.16)

$$\frac{du_2}{dz} = -cu_2 - 1 + a_1 u_1(w_1 + q) + a_2 u_1. \tag{2.16}$$

Similar computations for the rest of (2.9) were carried out, and the scaled model was obtained in the following equations.

$$\begin{aligned}
\frac{du_1}{dz} &= u_2,\\
\frac{du_2}{dz} &= -cu_2 - 1 + a_1u_1(w_1+q) + a_2u_1,\\
\frac{dv_1}{dz} &= v_2,\\
\frac{dv_2}{dz} &= -cv_2 - a_1u_1(w_1+q) + (a_2+a_3+a_4)\,v_1,\\
\frac{dw_1}{dz} &= w_2,\\
\frac{dw_2}{dz} &= -cw_2 - a_3v_1 + (a_5+a_6+a_7)\,w_1,\\
\frac{dq}{dz} &= a_5w_1 + a_4v_1 - (a_2+a_8+a_9)\,q,\\
\frac{dr}{dz} &= a_8q + a_7w_1 - a_2r,\\
\frac{df}{dz} &= a_6w_1 + a_9q.
\end{aligned} \tag{2.17}$$

Now, solving (2.17) simultaneously yielded two fixed points, the disease-free fixed point and the endemic fixed point in (2.18) and (2.19), respectively.

$$\begin{pmatrix} u_1^*\\ v_1^*\\ w_1^*\\ q_1^*\\ r_1^*\\ f_1^* \end{pmatrix} = \begin{pmatrix} \frac{1}{a_2}\\ 0\\ 0\\ 0\\ 0\\ 0 \end{pmatrix}, \tag{2.18}$$

$$\begin{pmatrix} u_2^*\\ v_2^*\\ w_2^*\\ q_2^*\\ r_2^*\\ f_2^* \end{pmatrix} = \begin{pmatrix} \frac{a_1a_9mnd}{a_1a_2a_9mnd+(a_1a_3d-a_2a_9mn)d}\\ \frac{a_1a_3d-a_2a_9mn}{a_1a_3md}\\ \frac{a_1a_3d-a_2a_9mn}{a_1mnd}\\ \frac{-a_6(a_1a_3d-a_2a_9mn)}{a_1a_9mnd}\\ \frac{(a_1a_3d-a_2a_9mn)(a_7a_9-a_6a_8)}{a_1a_2a_9mnd}\\ 0 \end{pmatrix}. \tag{2.19}$$

2.4.1. *Stability at the disease-free fixed point with diffusion speed.* At the disease-free fixed point, the basic reproduction number is determined by using the next generation matrix (NGM).

$$J = \begin{pmatrix} 0 & 1 & 0 & 0 & 0 & 0 & 0 & 0\\ a_1(w_1+q)+a_2 & -c & 0 & 0 & a_1u_1 & 0 & a_1u_1 & 0\\ 0 & 0 & 0 & 1 & 0 & 0 & 0 & 0\\ -a_1(w_1+q) & 0 & m & -c & -a_1u_1 & 0 & -a_1u_1 & 0\\ 0 & 0 & 0 & 0 & 0 & 1 & 0 & 0\\ 0 & 0 & -a_3 & 0 & n & -c & 0 & 0\\ 0 & 0 & a_4 & 0 & a_5 & 0 & -p & 0\\ 0 & 0 & 0 & 0 & a_7 & 0 & a_8 & -a_2 \end{pmatrix},$$

$$det(J) = \left|J - \lambda I\right| = 0,$$

$$\Rightarrow \begin{vmatrix} -\lambda & 1 & 0 & 0 & 0 & 0 & 0 & 0 \\ a_1(w_1+q)+a_2 & -c-\lambda & 0 & 0 & a_1u_1 & 0 & a_1u_1 & 0 \\ 0 & 0 & -\lambda & 1 & 0 & 0 & 0 & 0 \\ 0 & 0 & m & -c-\lambda & -a_1u_1 & 0 & -a_1u_1 & 0 \\ 0 & 0 & 0 & 0 & -\lambda & 1 & 0 & 0 \\ 0 & 0 & -a_3 & 0 & n & -c-\lambda & 0 & 0 \\ 0 & 0 & a_4 & 0 & a_5 & 0 & -p-\lambda & 0 \\ 0 & 0 & 0 & 0 & a_7 & 0 & a_8 & -a_2-\lambda \end{vmatrix} = 0.$$

The basic reproduction number with diffusion speed c is derived in the analysis below. The scaled model in (2.17) has a disease-free fixed point $\mathcal{D} = (s^*, e^*, i^*, q^*, r^*, f^*) = \left(\frac{1}{a_2}, 0, 0, 0, 0, 0\right)$, where $S(0)$ represents the initial size of the population that is susceptible to COVID-19. The asymptotic stability of the disease-free fixed point will be analyzed using the NGM [9]. The matrices, $\mathcal{F}$ and $\mathcal{V}$, representing new infection terms and the transition terms, respectively, are given by

$$\mathcal{F} = \begin{pmatrix} 0 & 0 & 0 & 0 & 0 \\ 0 & 0 & -\frac{a_1}{a_2} & 0 & -\frac{a_1}{a_2} \\ 0 & 0 & 0 & 0 & 0 \\ 0 & 0 & 0 & 0 & 0 \\ 0 & 0 & 0 & 0 & 0 \end{pmatrix}, \quad \mathcal{V} = \begin{pmatrix} 0 & 1 & 0 & 0 & 0 \\ m & -c & 0 & 0 & 0 \\ 0 & 0 & 0 & 1 & 0 \\ -a_3 & 0 & n & -c & 0 \\ a_4 & 0 & a_5 & 0 & -p \end{pmatrix},$$

$$\mathcal{F}\mathcal{V}^{-1} = \begin{pmatrix} 0 & 0 & 0 & 0 & 0 \\ 0 & 0 & -\frac{a_1}{a_2} & 0 & -\frac{a_1}{a_2} \\ 0 & 0 & 0 & 0 & 0 \\ 0 & 0 & 0 & 0 & 0 \\ 0 & 0 & 0 & 0 & 0 \end{pmatrix} \times \begin{pmatrix} 0 & 1 & 0 & 0 & 0 \\ m & -c & 0 & 0 & 0 \\ 0 & 0 & 0 & 1 & 0 \\ -a_3 & 0 & n & -c & 0 \\ a_4 & 0 & a_5 & 0 & -p \end{pmatrix}^{-1},$$

$$\mathcal{F}\mathcal{V}^{-1} = \begin{pmatrix} 0 & 0 & 0 & 0 & 0 \\ -\frac{a_1(a_4cn+a_3cp+a_3a_5c)}{a_2mnp} & -\frac{a_1(a_4n+a_3p+a_3a_5)}{a_2mnp} & -\frac{a_1(a_5c+cp)}{a_2np} & -\frac{a_1(a_5+p)}{a_2np} & \frac{a_1}{a_2p} \\ 0 & 0 & 0 & 0 & 0 \\ 0 & 0 & 0 & 0 & 0 \\ 0 & 0 & 0 & 0 & 0 \end{pmatrix},$$

$$\mathcal{R}_o = \left|-\frac{a_1(a_4cn+a_3cp+a_3a_5c)}{a_2mnp}\right|. \tag{2.20}$$

2.4.2. *Stability at the disease-free fixed point without diffusion speed.* The basic reproduction number without diffusion speed c was also derived using the following technique:

$$\begin{pmatrix} a_1(w_1+q)+a_2 & 0 & a_1u_1 & a_1u_1 & 0 \\ 0 & m & -a_1u_1 & -a_1u_1 & 0 \\ 0 & -a_3 & n & 0 & 0 \\ 0 & a_4 & a_5 & -p & 0 \\ 0 & 0 & a_7 & a_8 & -a_2 \end{pmatrix},$$

$$\mathcal{F} = \begin{pmatrix} 0 & 0 & 0 \\ 0 & -\frac{a_1}{a_2} & -\frac{a_1}{a_2} \\ 0 & 0 & 0 \end{pmatrix}, \quad \mathcal{V} = \begin{pmatrix} 0 & 0 & 0 \\ m & 0 & 0 \\ -a_3 & n & 0 \end{pmatrix},$$

$$\mathcal{F}\mathcal{V}^{-1} = \begin{pmatrix} 0 \\ 0 \\ -\frac{a_1(a_4 n + a_3 p + a_3 a_5)}{a_2 mnp} \end{pmatrix},$$

$$\mathcal{R}_o = \frac{\alpha\beta\left(\sigma(\psi+\delta+\kappa)+\gamma(\mu+\epsilon+\psi+\omega)\right)}{\mu(\epsilon+\mu+\omega)(\gamma+\mu+\sigma)(\psi+\delta+\kappa)}. \tag{2.21}$$

Similarly,

$$det(J) = \left|J - \lambda I\right| = 0,$$

$$\Rightarrow \begin{vmatrix} (a_1(w_1+q)+a_2)-\lambda & 0 & a_1u_1 & a_1u_1 & 0 \\ 0 & m-\lambda & -a_1u_1 & -a_1u_1 & 0 \\ 0 & -a_3 & n-\lambda & 0 & 0 \\ 0 & a_4 & a_5 & -p-\lambda & 0 \\ 0 & 0 & a_7 & a_8 & -a_2-\lambda \end{vmatrix} = 0.$$

The eigenvalues determined at the Jacobian matrix are

$$\begin{aligned} \lambda &= (a_1(w_1+q)+a_2) > 0, \\ \lambda &= m > 0, \\ \lambda &= n > 0, \\ \lambda &= -p < 0, \\ \lambda &= -a_2 < 0. \end{aligned}$$

Clearly, the Jacobian matrix without the speed c has three of its eigenvalues positive, whereas two of the real parts of the eigenvalues are negative, which indicates an unstable system. Thus, by making the unstable system stable, the method of Routh-Hurwitz was adapted.

The characteristic equation for the Jacobian matrix above is given by

$$P(\lambda) = \lambda^5 + B\lambda^4 + G\lambda^3 + H\lambda^2 + K\lambda + Y = 0. \tag{2.22}$$

2.4.3. *The Routh-Hurwitz stability criterion.* The Routh-Hurwitz criterion is used to tune variable parameters in order to keep the system in its stable state. Here, the coefficients of the characteristic equation are ordered into an array, also known as the Routh array. If the values in the first column are positive, then the system is stable.

Given that

$$\begin{aligned} B &= p - n - m - a_1(q+w_1), \\ G &= [a_1(m+n-p) - a_1a_2](q+w_1) - [a_1(a_3-a_4)]u_1 + m(n-p) - np, \\ H &= [a_1(mp+np-mn) - a_1a_2(m+n-p)](q+w_1) - [a_1a_4n + a_1a_3(p+a_5)]u_1 + mnp, \\ K &= [a_1a_2(mp+np-mn) - a_1mnp](q+w_1), \\ Y &= -a_1a_2mnp(q+w_1), \end{aligned}$$

from (2.22). Then the characteristic equation in (2.22) is summarized into the Routh array, which yielded the results below.

$$B > 0; \quad \frac{BG-H}{B} > 0; \quad H - \left(\frac{B(BK-Y)}{BG-H}\right) > 0.$$

2.5. **Global stability analysis of the model.** The global stability of the endemic fixed point of the scaled system with Dirichlet boundary conditions is established in this subsection. This is possibly done by constructing Lyapunov functionals for the state populations. Thus, the constructed Lyapunov functionals for the model are found based on the following theorems [10].

Theorem 2.5. *Let $x(t) = (s(t), e(t), i(t), q(t), r(t), f(t))$. Suppose $\dot{L}(x) = f(x)$ has a fixed point x^*; then the Lyapunov function with the two conditions is required.*

(1) $L(x(t)) > 0$, $\forall\ x$ on Ω in R^n and $x \neq x^*$,
(2) $\dot{L}(x(t)) < 0\ \forall\ x \in \Omega$ and $x \neq x^*$.

Remark 2.6. The definition for the first condition yields the following inequalities:

$$L(x(t)) = s^*\left(\frac{s}{s_2^*} - \ln\frac{s}{s_2^*}\right)e_2^*\left(\frac{e}{e_2^*} - \ln\frac{e}{e_2^*}\right) + a_5 i^*\left(\frac{i}{i_2^*} - \ln\frac{i}{i_2^*}\right) + q_2^*\left(\frac{q}{q_2^*} - \ln\frac{q}{q_2^*}\right) + \frac{a_6}{n}r_2^*\left(\frac{r}{r_2^*} - \ln\frac{r}{r_2^*}\right) > 0,$$

$$L(x(t)) = \left(s - s_2^*\ln\frac{s}{s_2^*}\right)\left(e - e_2^*\ln\frac{e}{e_2^*}\right) + a_5\left(i - i_2^*\ln\frac{i}{i_2^*}\right) + \left(q - q_2^*\ln\frac{q}{q_2^*}\right) + \frac{a_6}{n}\left(r - r_2^*\ln\frac{r}{r_2^*}\right) > 0.$$

Remark 2.7. The definition for the second condition gives the inequality below

$$\dot{L}(x(t)) = \frac{\partial L}{\partial s}\times\frac{ds}{dt} + \frac{\partial L}{\partial e}\times\frac{de}{dt} + \frac{\partial L}{\partial i}\times\frac{di}{dt} + \frac{\partial L}{\partial q}\times\frac{dq}{dt} + \frac{\partial L}{\partial r}\times\frac{dr}{dt} + \frac{\partial L}{\partial f}\times\frac{df}{dt} < 0.$$

Then the Lyapunov function constructed at the endemic fixed point requires the two conditions in order to be asymptotically stable [10].

Theorem 2.8. *Let $L(u)$ be a C^1 function defined on some domain in R^m, where $u(t)$ is a solution of the scaled equations in (2.17). Computing the time derivative of $L(u(t))$, then*

$$\frac{dL(u(t))}{dt} = \nabla L(u).f(u), \tag{2.23}$$

and set

$$W = \int_\Omega L(u(t,x))dx, \tag{2.24}$$

where (2.24) is the Lyapunov functional constructed for the model. By calculating the derivative across the positive solution of the model, set

$$\frac{dW}{dt} = \int_\Omega \nabla L(u).f(u)dx + \sum_{i=1}^{n} D_i\int_\Omega \frac{\partial L}{\partial u_i}\Delta u_i dx,$$

$$\frac{dW}{dt} = \int_\Omega a_8 q^*\left(4 - \frac{q}{q^*} - \frac{q^*}{q} - \frac{r}{r^*} - \frac{r^*}{r}\right) + a_2 r^*\left(5 - \frac{q^*}{q} - \frac{qr^*s}{q^*rs^*} - \frac{qr^*e}{q^*re^*} - \frac{qr^*i}{q^*ri^*} - \frac{rs^*e^*i^*}{r^*sei}\right)dx$$
$$- \left(\frac{s^*e^*i^*}{a_2a_3}\int_\Omega \frac{|\nabla s|^2}{s^2} + \frac{|\nabla e|^2}{e^2} + \frac{|\nabla i|^2}{i^2}\right)dx.$$

Hence,

$$\frac{dW}{dt} \leq 0.$$

It follows that W is a Lyapunov functional of the scaled model at the endemic fixed point $(s^*, e^*, i^*, q^*, r^*)$ and that it is valid for the conditions.

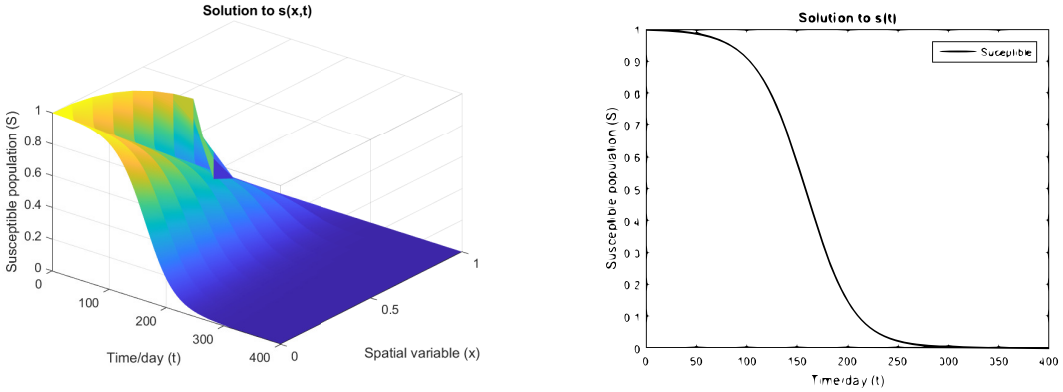

FIGURE 2. Plots of 3-D and 2-D for susceptible.

3. Numerical Results and Discussion

The results and findings of this study are presented in phase plots of the nonlinear differential equations of the population states in (2.7) [6]. These plots discussed in this section were plotted by using the data presented in Table 3 and the finite difference methods (FDM). Plots of the spatially dependent population states ($S, E,$ and I) are first presented in the first three figures, while those of the states that do not depend on space but only time *i.e.* ($Q, R,$ and$F$) are presented in the last plot.

3.1. **Plots of the susceptible population.** Figure 2 represents the three dimensional (3-D) and corresponding two dimensional (2-D) plots of the susceptible population. It can be observed from the 3-D plot that, from the onset of the outbreak of the disease, that is, between the times 0 and 100 days, the susceptible population was at its peak but started declining from 200 days. The deep blue color indicates the decrease in the susceptible population. This can be inferred from the compartmental model in the flowchart that the susceptible compartment loses to both the exposed class and natural death and gains from new births. Although there are newborn individuals being added to the susceptible class on a daily basis, the susceptible population decreases drastically at the expense of the new births as they (susceptible persons) interact with infectious persons. Again, as susceptible individuals travel throughout the domain, there is a constant spread of coronavirus within the domain, hence losing susceptible persons to the exposed class.

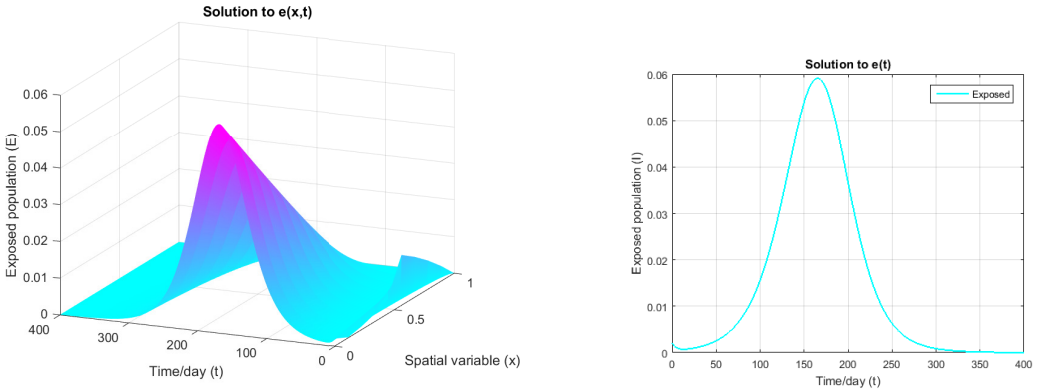

FIGURE 3. Plots of 3-D and 2-D for exposed.

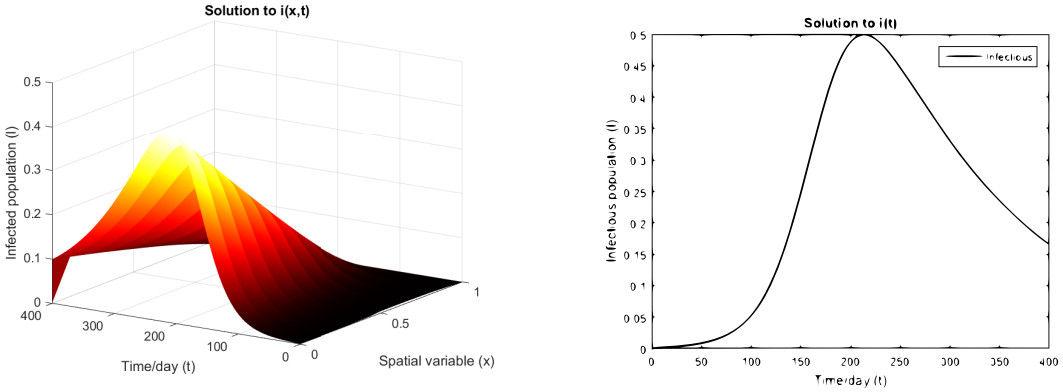

FIGURE 4. Plots of 3-D and 2-D for infectious.

3.2. **Plots of the exposed population.** Figure 3 is the phase plots of the exposed state. These figures are in purple and mint, as shown above. At the initial time of the outbreak, there are fewer infections of the disease. Between 100 and 200 days, the infection was at its peak, indicating a large proportion of the susceptible population had been exposed to COVID-19. Again, as time increases, the curve declines and falls flat, which implies the exposed population decreases as a result of losing to the infectious population or natural death. Making inferences from the compartmental diagram in Figure 1 or (2.7), the exposed population gains infected persons from the susceptible and has three losses to infectious, quarantined classes and natural death by the rates.

3.3. **Plots of the infectious population.** It can be observed from the time and space axes of the plot in Figure 4, the infectious figure, that there were no infections at time zero and space zero (no movement). However, as time started to increase, the infection became prevalent and peaked between the times of 200 and 300 days. The darker color indicates no disease, while the brighter color signifies the spread of the disease. Referring to the compartmental diagram in Figure 1 again, it can be seen that the infectious population losses to three other populations, $Q, R,$ and F. Nevertheless, the one gain from E is a negative gain. Thus, the I state tends to have massive loss as compared to S and E. After 300 days, the curve does not decline completely since, at this time, there are still infectious persons in Ghana.

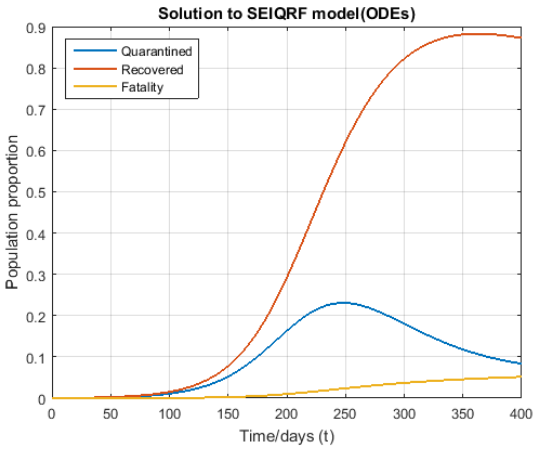

FIGURE 5. Plot of the quarantined, recovered, and fatality states.

TABLE 2. Initial conditions of the states and their proportions.

State	Description	Initial Population	Population at risk	Proportion
$S(0)$	Initial susceptible individuals	31,072,940	31,072,940	0.995889
$E(0)$	Initial exposed individuals	64,630	64,630	0.002071
$I(0)$	Initial infected individuals	5,358	5,358	0.000172
$Q(0)$	Initial quarantined individuals	0	920	0.000029
$R(0)$	Initial recovered individuals	0	56955	0.001825
$F(0)$	Initial deceased individuals	0	398	0.000013

TABLE 3. Initial values of the parameters.

Symbols	Description	Initial value
α	New birth rate	0.00007162
β	Transmission rate from infected persons	0.5500
γ	Rate at which exposed persons move into the infectious class	0.0714
σ	Rate at which exposed persons get self-isolation	0.9900
ψ	Rate at which detected infected persons are quarantined	0.0002
ϵ	Recovery rate of being quarantined	0.2000
κ	Recovery rate without being quarantined	0.9944
δ	Disease-induced death rate from infectious class	0.0500
ω	Disease-induced death rate from quarantined class	0.0056
μ	Natural death rate	0.00007868

3.4. **Plot of the quarantined, recovered, and fatality states.** Before the onset of the outbreak in Ghana, there had not been any quarantined individuals, nor any recoveries or deaths from COVID-19. Figure 5 depicts this dynamic. As the infection increased, patients with COVID-19 were put into mandatory quarantine. Many patients also responded to treatment and recovered, while the death curve in yellow gradually increased.

4. CONCLUSION

The study developed a new SEIQRF model with a constant diffusion term in Ghana. This model is a modification of the usual SIR and SEIR models that some authors used to describe the dynamics of COVID-19 [12, 17]. The diffusion term is incorporated in one dimension. The local stability analysis gave the qualitative solution to the model. This analysis explained how the basic reproduction number could be calculated at the disease-free fixed point. Also, the global stability analysis, however, was carried out at the endemic fixed points.

A study by [1] used a method of the Lyapunov functionals by constructing a delay partial differential equation. This study, however, focused on two conditions for the Lyapunov functionals using the Dirichlet boundary conditions. The findings from the global stability analysis indicate that the system is globally asymptotically stable at the endemic fixed point, which concludes that COVID-19 can be under control for a longer period of time. Both analyses ascertained relevant conclusions for this study, as the approximate value of the $R_0 = 3$ can help inform about how an infectious person is capable of infecting three more susceptible individuals. Though it is assumed that recovered persons cannot get reinfected.

For future studies, it is recommended that researchers modify this work by studying the bifurcation analysis of COVID-19, as many forms like the Omicron and Delta variants keep emerging and infecting the susceptible population. They can also consider the diffusion aspect in two or more dimensions as well as consider modeling using time-fractional diffusion equations.

5. Declaration of Competing Interest

The authors declare that there are no known competing financial or other interests that could have appeared to influence this work.

6. Data Availability

The COVID-19 data from March 2020 to February 2022 from Ghana Health Service were used, which are available at [7]. The data used were initial conditions of the population states in Ghana. The proportions of the population states and some parameter values were estimated as in [5]. Some predicted values of the parameters depending on their base values as used in [19] were used.

Acknowledgment

We acknowledge the contributions of Benedict Barnes to this research.

References

[1] M. Ali, M. Imran, and A. Khan, *Analysis and prediction of the COVID-19 outbreak in pakistan*, Journal of Biological Dynamics, *14*(1) (2020), 730–747.
[2] J. K. K. Asamoah, M. A. Owusu, Z. Jin, F.T. Oduro, A. Abidemi, and E. O. Gyasi, *Global stability and cost-effectiveness analysis of COVID-19 considering the impact of the environment: using data from Ghana*, Chaos, Solitons and Fractals, *140* (2020), 110103.
[3] N. Bacaër, *Mckendrick and kermack on epidemic modelling (1926–1927)*, A Short History of Mathematical Population Dynamics, (2011), 89–96.
[4] F. Brauer, *The kermack–mckendrick epidemic model revisited*, Mathematical biosciences, *198*(2) (2005), 119–131.
[5] S. Y. Chae, K. Lee, H. M. Lee, N. Jung, Q. A. Le, B. J. Mafwele, T. H. Lee, D. H. Kim, and J. W. Lee, *Estimation of infection rate and predictions of disease spreading based on initial individuals infected with COVID-19*, Frontiers in Physics, *311* (2020).
[6] R. S. Esfandiari, *Numerical methods for engineers and scientists using MATLAB®*, Crc Press, (2017).
[7] Ghana Health Service, E. Kenu, Ghana COVID-Coronavirus Statistics-Worldometer 2020 Accessed 31st may, 2020, https://www.worldometers.info/coronavirus/.
[8] Ghana Health Service, COVID-19 Updates—Ghana. Retrieved 31st may, 2020, https://ghs.gov.gh/covid19/archive_2020.php.
[9] N. Hartemink, S. Randolph, S. Davis, and J. Heesterbeek, *The basic reproduction number for complex disease systems: Defining r 0 for tick-borne infections*, The American Naturalist, *171*(6) (2008), 743–754.
[10] K. Hattaf and N. Yousfi, *Global stability for reaction–diffusion equations in biology*, Computers & Mathematics with Applications, *66*(8) (2013), 1488–1497.
[11] S. H. Khoshnaw, M. Shahzad, M. Ali, and F. Sultan, *A quantitative and qualitative analysis of the covid–19 pandemic model*, Chaos, Solitons and Fractals, *138* (2020), 109932.
[12] L. Li, Z. Yang, Z. Dang, C. Meng, J. Huang, H. Meng, D. Wang, G. Chen, J. Zhang, H. Peng, and Y. Shao, *Propagation analysis and prediction of the COVID-19*, Infectious Disease Modelling, *5* (2020), 282–292.
[13] P. Mo, Y. Xing, Y. Xiao, L. Deng, Q. Zhao, H. Wang, Y. Xiong, Z. Cheng, S. Gao, K. Liang, M. Luo, T. Chen, S. Song, Z. Ma, X. Chen, R. Zheng, Q. Cao, F. Wang, and Y. Zhang, *Clinical characteristics of refractory COVID-19 pneumonia in wuhan, china*, Clinical Infectious Diseases, (2020).
[14] C. J. Murray and A. D. Lopez, *Global mortality, disability, and the contribution of risk factors: Global burden of disease study*, The lancet, *349*(9063) (1997), 1436–1442.
[15] J. D. Murray, *Mathematical biology II: spatial models and biomedical applications*, Springer New York, *3* (2001).
[16] F. Ndaïrou, I. Area, J. J. Nieto, and D. F. Torres, *Mathematical modeling of COVID-19 transmission dynamics with a case study of wuhan*, Chaos, Solitons and Fractals, *135* (2020), 109846.

[17] K. Prem, Y. Liu, T. W. Russell, A. J. Kucharski, R. M. Eggo, and N. Davies, *The effect of control strategies to reduce social mixing on outcomes. of the COVID-19 epidemic in wuhan, china: a modelling study*, The Lancet Public Health, *5*(5) (2020), e261–e270.
[18] J. Wang, *Mathematical models for COVID-19: applications, limitations, and potentials*, Journal of public health and emergency, *4*(9) (2020).
[19] I. M. Wangari, S. Sewe, G. Kimathi, M. Wainaina, V. Kitetu, and W. Kaluki, *Mathematical modelling of COVID-19 transmission in Kenya: a model with reinfection transmission mechanism*, Computational and Mathematical Methods in Medicine, (2021), 5384481.
[20] J. Wen, C. C. Wang, and M. Kozak, *Post-COVID-19 Chinese domestic tourism market recovery: potential influence of traditional Chinese medicine on tourist behaviour*, Anatolia, *32*(1) (2021), 121–125.
[21] T. D. Wickens, *Elementary signal detection theory*, Oxford university press, 2001.
[22] H. Yao, Y. Song, Y. Chen, N. Wu, J. Xu, C. Sun, J. Zhang, T. Weng, Z. Zhang, Z. Wu, L. Cheng, D. Shi, X. Lu, J. Lei, M. Crispin, Y. Shi, L. Li, and S. Li, *Molecular architecture of the SARS-CoV-2 virus*, Cell, *183*(3) (2020), 730–738.
[23] S. P. Zhang, Y. R. Yang, and Y. H. Zhou, *Traveling waves in a delayed SIR model with nonlocal dispersal and nonlinear incidence*, Journal of Mathematical Physics, *59*(1) (2018), 011513.